Boundary conditions for magnetization in magnetic nanoelements

K. Yu. Guslienko[1,*] and A. N. Slavin[2]
[1]*Materials Science Division, Argonne National Laboratory, Argonne, Illinois 60439, USA*
[2]*Department of Physics, Oakland University, Rochester, Michigan 48309, USA*
(Received 16 May 2005; published 27 July 2005)

We show that the dynamic magnetization at the edges of a thin magnetic element with a finite lateral size can be described by new effective boundary conditions that take into account inhomogeneous demagnetizing fields near the element edges. These fields play a dominant role in the effective pinning of the dynamic magnetization at the boundaries of mesoscopic- and nanosized magnetic elements. The derived effective boundary conditions generalize well-known Rado-Weertman boundary conditions and are reduced to them in the limiting case of a very thin magnetic element.

DOI: 10.1103/PhysRevB.72.014463 PACS number(s): 75.75.+a, 75.30.Ds, 75.40.Gb

Rapid progress in magnetic data recording and sensor technologies creates a motivation to work with submicron magnetic elements.[1] The physics of mesoscopic and nanomagnetic elements is qualitatively different from that of bulk magnetic systems. The confinement of spin wave modes and other finite-size effects dominate the properties of magnetic nanoparticles[2,3] and create opportunities for novel applications in spintronic devices.[4,5] The use of small magnetic elements in data recording[4,6] or for current-induced microwave generation and switching[5,6] depends on our understanding of their fundamental dynamical properties.

The central problem is to understand the dipole-dipole interaction and its interplay with other factors, including the exchange interaction and surface anisotropy. When the relevant interactions are properly taken into account, it is possible to calculate the excitation spectra of the magnetic elements in terms of spin wave eigenmodes. These spectra provide information on the characteristic times of magnetization reversal as studied experimentally,[7,8] and provide much needed general insights. The magnetization (**M**) dynamics of a magnetic element can be described using the Landau-Lifshitz equation of motion. This approach contains contributions from the nonuniform exchange interaction, as well as from the long-range dipole-dipole interaction, which is also nonuniform for nonellipsoidal magnetic elements. The eigenfrequencies and eigenmode distributions of spin-wave excitations in such elements depend strongly on the boundary conditions at the element surfaces. Knowledge of these boundary conditions is important to calculate the spectra of magnetic linear excitations (spin waves) in the element, both in the case of a uniform ground state, when the element is magnetized by the external magnetic field to saturation, and in the case when the ground state is strongly nonuniform (e.g., a magnetic vortex).

It is known that the usual electrodynamic boundary conditions of the Maxwell classical theory leave the amplitude of the dynamic magnetization at the boundary undefined. Maxwell's theory requires the continuity of the normal components of the magnetic induction and the tangential components of the magnetic field. The problem is that the magnetic moments near the boundaries experience the influence of local magnetic fields that are different from the fields in the bulk. Kittel[9] introduced boundary conditions of total "pinning" ($\mathbf{M}=0$ at the boundary) based on Neel's concept of surface anisotropy[10] to explain experimental data on spin-wave resonances in magnetic films. General "exchange" boundary conditions for the dynamic magnetization were then formulated by Rado and Weertman (RW).[11] In addition to Kittel's term, RW took into account the influence of the exchange interaction, and obtained what is known as the Rado-Weertman boundary conditions:

$$L_e^2 \mathbf{M} \times \frac{\partial \mathbf{M}}{\partial n} + \mathbf{T}_s = 0, \tag{1}$$

where $L_e=(2A/M_s^2)^{1/2}$ is the characteristic exchange length of a material (defining the length scale at which the exchange interaction becomes important), A is the exchange stiffness, M_s is the saturation magnetization, $\partial/\partial n$ is the partial derivative along a unit vector **n** (an inward normal direction to the particle surface), and $\mathbf{T}_s$ is the sum of all the surface torques that arise from forces other than the exchange interaction. The term $\mathbf{T}_s$ usually contains contributions from the Neel surface anisotropy $\mathbf{T}_a$, but contributions from other local fields are also possible. The boundary conditions (1) generalize Kittel's, and permit both a totally "pinned" magnetization ($\mathbf{M}=0$) when the torque $\mathbf{T}_s$ is large, and also a pinning of an arbitrary magnitude up to the totally "free" or "unpinned" magnetization ($\partial\mathbf{M}/\partial n=0$) at the boundaries when $\mathbf{T}_s$ is small and the exchange interaction is dominant.

In the present article we demonstrate that to derive accurate boundary conditions for the dynamic magnetization at the lateral edges of a thin mesoscopic or nanosized magnetic element, it is not sufficient to take into account only the Neel surface anisotropy in the expression for $\mathbf{T}_s$, as it was done in the majority of previously published papers on this subject (see, e.g., Ref. 12 and references therein). It is also necessary to include a contribution from the strongly nonuniform internal dipolar field existing near the element edges. Then, the surface torque near the lateral edge of the element in Eq. (1) becomes $\mathbf{T}_s=\mathbf{T}_a+\mathbf{T}_m$, where the second dipolar (magnetostatic) term can be dominant in a certain range of the element thickness L. To take into account the dipolar field, it is convenient to rewrite Eq. (1) in the form:

$$\mathbf{M} \times \left(L_e^2 \frac{\partial \mathbf{M}}{\partial n} - \nabla_M E_a + \mathbf{H}_m L \right) = 0, \qquad (2)$$

where $E_a(\mathbf{M})$ is the energy density of the surface anisotropy, and $\mathbf{H}_m$ is the dipolar field near the element edge, and L is the element thickness.

Below we use Eq. (2) to derive the explicit form of boundary conditions at the lateral edges of thin magnetic elements ($L \leqslant w, R$), where w and R are the in-plane sizes of elements having either a rectangular or cylindrical shape. We also assume that at the face surfaces of the magnetic element at a distance from the edge of the order of the element thickness L the influence of the inhomogeneous dipolar field is negligible, and the RW boundary conditions[11] determined only by the surface anisotropy and exchange interaction can be applied. For simplicity, we consider only the case of a uniaxial surface anisotropy with anisotropy constant K_s and the anisotropy axis direction given by a unit vector $\mathbf{n}_a$. The effective field of surface anisotropy is then given by $\mathbf{H}_a = -\nabla_M E_a = (2K_s/M_s^2)(\mathbf{M} \cdot \mathbf{n_a})\mathbf{n_a}$. Our main task is to evaluate the dipolar field $\mathbf{H}_m$ that exists near the lateral edges of a thin magnetic element.

In our calculation we represent the magnetization in Eq. (2) in the form $\mathbf{M} = M_s \mathbf{i}_0 + \mathbf{m}$, where $\mathbf{i}_0$ is a unit vector in the direction of the equilibrium magnetization $\mathbf{M}_s$. We assume that the dynamic magnetization $\mathbf{m}$ is perpendicular to $\mathbf{M}_s$ or $\mathbf{m} \cdot \mathbf{i}_0 = 0$, and that its magnitude m is much smaller than the M_s ($m \ll M_s$), which is correct for any linear magnetic excitations. In a thin in-plane magnetized element made of a *soft* magnetic material, vector $\mathbf{i}_0$ lies in the plane of the element, and is directed along its lateral edge to minimize the magnetostatic energy of the static magnetic configuration. Other directions of $\mathbf{i}_0$ are also possible, leading to some mathematical complications, which are not principal and will be considered elsewhere. The element could have an arbitrary shape. The only critical requirement is that it is thin, i.e., that the element thickness L is much smaller than the element lateral size. Typical shapes could be a thin rectangular prism or a thin circular or elliptical cylinder. Submicron plane magnetic dots prepared by lithographic patterning of thin magnetic films made of Fe, Co, or NiFe are good examples of such thin magnetic elements.[8,13,14] Dipolar boundary conditions for particular case of thin magnetic rectangular stripes were explicitly calculated in Ref. 15 and successfully applied for a quantitative interpretation of Brillouin light scattering experiments.

In practical calculations of spin wave spectra in thin magnetic elements, it is usually assumed that the dynamic magnetization at the edges is totally pinned, as is described by Kittel's boundary conditions (see, e.g., Ref. 16). This approach, however, is rather arbitrary, and is not based on an exact knowledge of the behavior of the dynamic magnetization near the boundary. To derive boundary conditions for a thin magnetic element we evaluate the inhomogeneous dipolar field $\mathbf{H}_m$ directly from the Maxwell's equations. For mathematical simplicity we consider a case of an axially magnetized stripe with a rectangular cross section (see Fig. 1), which has only *one finite lateral caliper* (width w). The general solution of Maxwell's equations for the dipolar field

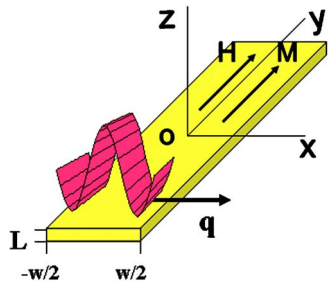

FIG. 1. (Color online) Coordinates system for a thin magnetic stripe.

$\mathbf{H}_m$ can be written as a sum of two fields $\mathbf{H}_m(\mathbf{r}) = \mathbf{H}_S(\mathbf{r}) + \mathbf{H}_V(\mathbf{r})$, resulting from surface (S) and volume (V) magnetic charges:[17]

$$\mathbf{H}_m(\mathbf{r}) = -\nabla_{\mathbf{r}} \int dS \frac{m_n(\mathbf{r}')}{|\mathbf{r} - \mathbf{r}'|} + \nabla_{\mathbf{r}} \int dV \frac{\nabla_{\mathbf{r}'} \cdot \mathbf{m}(\mathbf{r}')}{|\mathbf{r} - \mathbf{r}'|}. \qquad (3)$$

We evaluate the dipolar field (3) for an infinitely long magnetic stripe having thickness L, uniformly magnetized along the y axis, while the z axis is directed along the stripe thickness (see Fig. 1). The boundary conditions for magnetization in a stripe can be written as projections of the vector torque equation (2) on the coordinate axes. Since the stripe is infinite in the y direction, the distribution of the dynamic magnetization $\mathbf{m}(\mathbf{r}) = \mathbf{m}(x,z)$ within the stripe and the demagnetizing field $\mathbf{H}_m(\mathbf{r}) = \mathbf{H}_m(x,z)$ are independent of the coordinate y, and y components of both these vectors are vanishing. We also assume a homogeneous distribution of the dynamic magnetization along the coordinate z [making $\mathbf{m}(\mathbf{r}) = \mathbf{m}(x)$], since we consider thin magnetic elements with the thickness of the order of L_e. For the case of a thin magnetic stripe with aspect ratio $p = L/w \ll 1$ and the situation when $\mathbf{m}(\mathbf{r}) = \mathbf{m}(x)$, the torque (2) and the dipolar field (3) have only x and z components, and can be simplified. At first, we consider only the x component $H_{mx}(\mathbf{r})$ of the dipolar field (3). Since we are interested in the boundary conditions at the lateral edges of the stripe (the planes $x = \pm w/2$ in Fig. 1), we can also average the x component of the dipolar field (3) over the coordinate z, making it a function of the coordinate x only: $h(x) = \langle H_{mx}(x,z) \rangle_z$. We separate the contributions from the surface and volume magnetic charges, and write $h(x) = h_S(x) + h_V(x)$. Note, that at the lateral surface $x = w/2$, the surface charges are given by $m_x(w/2)$ and the volume charges are defined by $\partial m_x(x)/\partial x$.

An evaluation of the integrand in the first (surface) integral in (3) at the face surfaces ($z = 0, L$) of the stripe shows that the face surface magnetic charges (proportional to m_z) do not contribute to the x component of the dipolar field $h(x)$.[15] An evaluation of the same integrand at the lateral ($x = \pm w/2$) surfaces of the stripe yields the dipolar field $h_S(x) = \{2\pi\theta(x - w/2) + F[(w/2 - x)/L]\} m_x(w/2)$, where $\theta(x) = \text{sign}(x)$ and $F(\eta) = 2\eta \ln(1 + 1/\eta^2) + 4 \tan^{-1} \eta$. A direct calculation shows that near the lateral boundary $x = w/2$ of the stripe, the contribution of the second term in the expression for $h_S(x)$ is small (of the order of the stripe aspect ratio p).

Only the first term of $h_S(x)$ gives a contribution (of the order of 2π) to the boundary conditions in the main approximation. In the calculation of the dipolar field $h_S(x)$ near the right $x \approx w/2$ lateral surface of the stripe, we neglect the contribution to it from the surface charges at the left lateral surface $x=-w/2$, and *vice versa*.

To evaluate the second (volume) integral in (3) near the lateral boundary of the stripe, we expand the variable magnetization $\mathbf{m}(x)$ in a Taylor series. Only the x component of the variable magnetization is important in this case, and that the main contribution to the dipolar field $h_V(x)$ comes from term containing the first spatial derivative of m_x. This yields the "volume" dipolar field in the form $h_V(x) = wI(x,p)\partial m_x(x)/\partial x$, where near the boundary $x=w/2$ the function $I(x,p)$ is evaluated as $I(w/2,p)=p-2p\ln p$.[15] All other terms in the field $h_V(x)$, containing higher-order derivatives $\partial^s m_x(x)/\partial x^s$ $(s>1)$, in the limit of a thin stripe $p \ll 1$ are substantially smaller than the first term.[15] A similar situation exists at the other lateral boundary $x=-w/2$. Substituting the calculated expressions of $h(x)=h_S(x)+h_V(x)$ for $\mathbf{H}_m$ in Eq. (2), we get the following relations between the x component of $\mathbf{m}$ and its first derivative at the stripe boundaries $x=w/2-0$ and $x=-w/2+0$:

$$\pm \frac{\partial m_x(\xi)}{\partial \xi} + d(p,L)\, m_x(\xi)\big|_{\xi=\pm 1/2} = 0. \tag{4}$$

These relations that can be interpreted as effective boundary conditions, where $d(p,L)$ is the effective "pinning" parameter and $\xi=x/w$ is the dimensionless coordinate perpendicular to the lateral boundary of the stripe. The direction of the normal n to the lateral surface of the stripe is defined as $\mathbf{n}=-x\mathbf{e}_x$, where $\mathbf{e}_x$ is the unit vector along the x axis. Similar boundary conditions can be obtained for the z component of the dynamic magnetization.

As an alternative example of a thin magnetic element we also considered a circular cylinder having thickness L and radius R $(L \ll R)$. We used an approach similar to that for a long rectangular stripe and obtained a result for the pinning parameter analogous to the result obtained for the stripe. A general expression for the pinning parameter in (4), which is correct in both rectangular and cylindrical geometry, can be written in the following form:

$$d(p,L) = \frac{2\pi\left[1-\left(\dfrac{K_s}{\pi M_s^2 L}\right)\right]}{p\left[a + b\ln(1/p) + \left(\dfrac{L_e}{L}\right)^2\right]}, \tag{5}$$

where the values of the coefficients a and b are determined by the geometry of the element $(a,b \sim 1)$, and the parameter p is the thickness to the lateral size aspect ratio of a thin magnetic element. In particular, $p=L/w$ for a stripe of the width w and $p=L/R$ for a circular cylinder of the radius R. Calculations yield the following values for the coefficients a and b: $a=1$, $b=2$ for a rectangular stripe, and $a=2(6\ln 2-1)$, $b=4$ for a circular cylinder.

The above-derived boundary conditions (4) with the effective pinning parameter (5) generalize the well-known RW boundary conditions[11] for the case of a thin magnetic element having a finite lateral size, and represent the main result of this paper. The sign of the pinning parameter in our definition (5) is *opposite* to the sign in the pinning parameter defined in Ref. 11, so that $d(p,L)>0$ in (5) corresponds to the "easy plane" type of *effective* surface anisotropy. The calculated pinning parameter (5) corresponds to a strong pinning if $w,R \gg L \geq L_e$ (dipolar dominated regime), and to a weak pinning if $(Lw)^{1/2} < L_e$ or $(LR)^{1/2} < L_e$ (exchange-dominated regime). We believe that although our calculations were done for rectangular and circular geometries, similar effective boundary conditions could be obtained in other geometries, in particular for a thin magnetic dot having the shape of an elliptical cylinder.

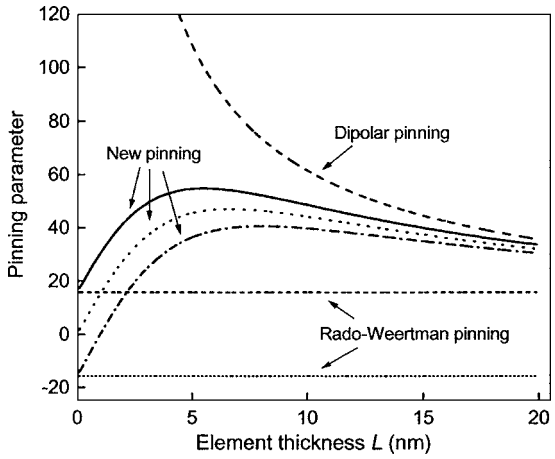

FIG. 2. Pinning parameter for a thin magnetic stripe vs stripe thickness L (the stripe width is $w=1000$ nm). The dashed line corresponds to pure dipolar pinning ($K_s=0$, $L_e=0$) of Ref. 15. The solid line corresponds to the easy-plane surface anisotropy ($K_s/\pi M_s^2=-1$ nm), while the dot-dashed line corresponds to the easy-axis type of surface anisotropy ($K_s/\pi M_s^2=1$ nm) [see Eq. (5)]. The dotted line corresponds to $K_s=0$, the horizontal lines correspond to Rado-Weertman pinning with $K_s/\pi M_s^2=-1$ nm (upper), and $K_s/\pi M_s^2=1$ nm (lower). $L_e=20$ nm.

The pinning parameter $d(p,L)$ calculated from Eq. (5) is shown in Fig. 2 as a function of the element thickness. The exchange interaction dominates for small L, and the pinning parameter decreases as the element thickness L decreases. In the case of a nonzero surface anisotropy, deviations of the pinning parameter (5) from the purely dipolar pinning[15] occur for the element thickness $L<10$ nm and are stronger for an "easy axis" type of surface anisotropy $(K_s>0)$ (see the dot-dashed line in Fig. 2). For this type of surface anisotropy, the pinning parameter (5) also strongly differs from the RW pinning due to the competing contributions from surface anisotropy and dipolar interaction. For $K_s=0$ the pinning (5) depends on the ratio L/L_e and is strong if $L/L_e>0.1$. For larger values of L, but still in the limit $p \ll 1$, the dipolar contribution to pinning becomes dominant independently of the sign and value of the surface anisotropy. The absolute value of $|K_s|=0.20$ erg/cm^2 used in Fig. 2 ($M_s=800$ G) corresponds to a relatively strong surface anisotropy. We note that for the majority of soft magnetic materials the contribution from the surface anisotropy to the effective pinning pa-

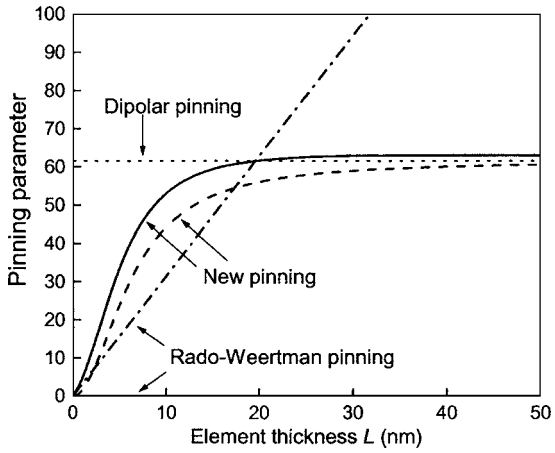

FIG. 3. Pinning parameter given by Eq. (5) for thin magnetic stripe vs element thickness L keeping the aspect ratio $p=0.01$ as constant. The dotted line corresponds to pure dipolar pinning ($K_s=0$, $L_e=0$). The solid line and the dashed line are for a surface anisotropy $K_s/\pi M_s^2=-2$ nm and $K_s=0$, respectively. The dashed-dotted line corresponds to RW pinning with the same parameters. $L_e=20$ nm.

rameter (5) can be neglected because usually $K_s \ll \pi L M_s^2$. Figure 3 demonstrates a crossing regime from the case of a strong dipolar pinning to the case of a weaker exchange-dominated pinning when the element thickness is decreased and the element aspect ratio p is kept constant (proportional scaling of the element's sizes). The pinning vanishes at $L \to 0$, which reflects the increasing role of the short-range exchange interaction. Note that the purely dipolar value of the pinning parameter $d(p)=2\pi p^{-1}[1+2\ln(1/p)]^{-1}$ derived in Ref. 15 and RW value of the pinning, $d_{RW}(p,L) = -2K_s L/pM_s^2 L_e^2$,[11] serve as two asymptotes for the pinning parameter given by Eq. (5). The first limiting value is achieved for $L > L_e$, while for the second limiting value we get $L < L_e$. It is also clear that the general pinning parameter (5), in the limit $L \to 0$, is equivalent to the RW pinning, independently of the sign of the surface anisotropy.

We stress, that, although the boundary conditions (4) look formally analogous to the exchange boundary conditions in a perpendicularly magnetized film, the effective pinning is actually a result of the interplay of the exchange, dipolar, and surface anisotropy terms. In contrast to the usual "exchange" pinning, the pinning parameter (5) is not fully determined by the surface anisotropy of the magnetic material. The physical role of this generalized pinning is to minimize the total surface energy (the sum of exchange, anisotropy, and magnetostatic energies). The magnetostatic part results from the induced surface charges $\sigma=(\mathbf{m}\cdot\mathbf{n})_S$ at the edges of finite-size nonellipsoidal magnetic element and volume charges near its edges. For $p \to 0$, the pinning parameter $d(p,L)$ of Eq. (5) is rather large, and the boundary conditions (4) are close to the Kittel's boundary conditions[9] that were traditionally used at the lateral edges of thin magnetic elements.[16] A more detailed analysis shows that in the boundary conditions (4) the term proportional to the dynamic magnetization $\mathbf{m}$ comes from the surface magnetic charges and surface anisotropy. The term proportional to the derivative $\partial m/\partial x$ comes from the volume magnetic charges (and exchange), if we retain only the main terms in the small parameter p. The strong pinning in the dipole-dominated regime corresponds to a large ratio of surface/volume charges, and for thin magnetic elements ($p \ll 1$) represents a "finite-size" effect.

The derived boundary conditions (4) are especially important within the thickness range 2–10 nm (see Figs. 2 and 3), where the pinning described by Eq. (5) differs significantly from the "dipolar" value given by horizontal line in Fig. 3 (see also Ref. 15). Our predictions can be tested in any dynamical experiments using magnetic elements with the aspect ratio $p \ll 1$ and $L \leqslant 10$ nm. In particular, for the conditions of the experiment,[7] where the "free" layer of a nanopillar driven by spin-polarized current has a shape of an elliptical cylinder with the sizes $3\times130\times70$ nm and is relatively thin ($L < L_e$), our equation (5) predicts negligible pinning at the lateral edge of the free layer, thus excluding the influence of the exchange interaction on the frequency of the lowest spin wave mode excited in the nanopillar. This conclusion is supported by the results of the experiment,[7] where the dependence of the current-induced microwave frequency on the bias magnetic field for the small precession angle regime is well described by the purely dipolar (nonexchange) expression for the quasihomogeneous precession mode of a nanopillar. At the same time, we would like to note that in the relatively thick magnetic elements of the thickness of $L=30-70$ nm ($L > L_e$) with the in-plane size of about w, $R=500-1000$ nm Eq. (5) predicts strong dipolar pinning for the lowest spin wave modes, and the spin wave frequencies calculated using the effective pinning parameter given by Eq. (5) are in good quantitative agreement with experiments performed in both circular[14,18] and rectangular[15] magnetic elements.

In summary, we derived general boundary conditions (4) with the *effective* pinning parameter (5) for the dynamic magnetization of thin magnetic nonellipsoidal elements. These conditions take into account exchange interaction, surface anisotropy, and a nonuniform dipolar field near the element lateral edges. The contribution of the dipolar field to the effective pinning parameter is dominant for the element thickness $L_e < L \ll w, R$, while for $L \to 0$ ($L_e > L > 0$) the exchange and surface anisotropy contributions become gradually more important, and our boundary conditions are reduced to the well-known Rado-Weertman form.[11] The derived boundary conditions (4) and (5) are important in the interpretation of spin wave spectra of nanosized magnetic elements, and are well supported by several independent experiments (see, e.g., Refs. 7, 14, and 15).

We would like to thank S. D. Bader for his useful and constructive comments on the manuscript. K.G. acknowledges support by the U.S. Department of Energy, BES Material Sciences under Contract No. W-31-109-ENG-38. The work of A. S. was supported by the Grant No. W911NF-04-1-0299 from the U.S. Army Research Office, by the MURI grant W-911NF-04-1-0247 from the Department of Defense, and by the Oakland University Foundation.

*Author to whom correspondence should be addressed. Electronic address: gusliyenko@anl.gov

[1] A. Thiaville and J. Miltat, Science **284**, 1939 (1999); J. Miltat and A. Thiaville, *ibid.* **290**, 466 (2000).

[2] C. Stamm, F. Marty, A. Vaterlaus, V. Weich, S. Egger, U. Maier, U. Ramsperger, H. Fuhrmann, and D. Pescia, Science **282**, 449 (1998).

[3] T. Shinjo, T. Okuno, R. Hassdorf, K. Shigeto, and T. Ono, Science **289**, 930 (2000).

[4] G. A. Prinz, Science **282**, 1660 (1998).

[5] M. Tsoi, J. Z. Sun, and S. S. P. Parkin, Phys. Rev. Lett. **93**, 036602 (2004).

[6] I. Tudosa, C. Stamm, A. B. Kashuba, F. King, H. C. Siegmann, J. Stoehr, G. Ju, B. Lu, and D. Weller, Nature (London) **428**, 831 (2004).

[7] S. Kiselev, J. C. Sankey, I. N. Krivorotov, N. C. Emley, R. J. Schoelkopf, R. A. Buhrman, and D. C. Ralph, Nature (London) **425**, 380 (2003).

[8] J. Jorzick, S. O. Demokritov, B. Hillebrands, M. Bailleul, C. Fermon, K. Yu. Guslienko, A. N. Slavin, D. V. Berkov, and N. L. Gorn, Phys. Rev. Lett. **88**, 047204 (2002).

[9] C. Kittel, Phys. Rev. **110**, 1295 (1958).

[10] L. Neel, J. Phys. Radium **15**, 225 (1954).

[11] G. T. Rado and J. R. Weertman, J. Phys. Chem. Solids **11**, 315 (1959).

[12] R. J. Hicken, G. T. Rado, G. Xiao, and C. L. Chien, Phys. Rev. Lett. **64**, 1820 (1990).

[13] C. Mathieu, J. Jorzick, A. Frank, S. O. Demokritov, A. N. Slavin, B. Hillebrands, B. Bartenlian, C. Chappert, D. Decanini, F. Rousseaux, and E. Cambril, Phys. Rev. Lett. **81**, 3968 (1998).

[14] G. N. Kakazei, P. E. Wigen, K. Yu. Guslienko, V. Novosad, A. N. Slavin, V. O. Golub, N. A. Lesnik, and Y. Otani, Appl. Phys. Lett. **85**, 443 (2004).

[15] K. Y. Guslienko, S. O. Demokritov, B. Hillebrands, and A. N. Slavin, Phys. Rev. B **66**, 132402 (2002).

[16] A. G. Gurevich and G. A. Melkov, *Magnetization Oscillations and Waves* (CRC Press, New York, 1996), Chap. 6.

[17] J. D. Jackson, *Classical Electrodynamics* (Wiley, New York, 1975).

[18] K. Y. Guslienko, W. Scholz, R. W. Chantrell, and V. Novosad, Phys. Rev. B **71**, 144407 (2005).